Climate Dynamics (2018) 51:3785–3796
https://doi.org/10.1007/s00382-018-4110-x

Signature of the South China Sea summer monsoon onset on spring-to-summer transition of rainfall in the middle and lower reaches of the Yangtze River basin

Xingwen Jiang[1,2] · Zunya Wang[3] · Zhenning Li[4]

Received: 1 September 2017 / Accepted: 21 January 2018 / Published online: 29 January 2018

Abstract
The South China Sea (SCS) summer monsoon onset has been regarded as the beginning of the East Asian summer monsoon. In this study, we investigated the impacts of the SCS monsoon onset on the transition from the spring persistent rainfall to the summer Meiyu in the middle and lower reaches of the Yangtze River basin (MLYZB). It is found that rainfall in the MLYZB reduces after the SCS monsoon onset. This reduction in rainfall persists until the onset of the Meiyu and is accompanied by a weakening of southwesterlies to the south of the MLYZB. These features exist in both climatology and interannual variability. Rainfall increases significantly over the SCS and the subtropical western North Pacific after the SCS monsoon onset. The latent heating of the increased rainfall can excite an anomalous cyclone over the western North Pacific, which weakens the mean southwesterlies to the south of the MLYZB and decreases water vapor entering the MLYZB. It also generates descending motion over southeastern China. Thus, the SCS monsoon onset could suppress rainfall over the MLYZB by the latent heating induced changes in circulation. Compared to increased rainfall over the SCS, the latent heating of increase rainfall over the subtropical western North Pacific plays a more important role in the reduction of rainfall over the MLYZB. As the SCS monsoon onset affects the timing of the reduction of rainfall in the MLYZB, an early SCS monsoon onset is accompanied by below-normal May rainfall in the MLYZB, while a late SCS monsoon onset is accompanied by above-normal May rainfall.

1 Introduction

The East Asia summer monsoon exhibits variability on a wide range of time scales (e.g. Ding and Chan 2005; Li et al. 2010; Ding et al. 2010). Its intraseasonal variability features the distinct stepwise northward advance from the tropics to middle latitudes (e.g. Ding and Chan 2005). After the South China Sea (SCS) summer monsoon onset, the monsoon related rain belt moves northward over East Asia; therefore, the SCS monsoon onset has been regarded as the commencement of the East Asian summer monsoon (Ding and Chan 2005; Wang et al. 2004) and many studies have been devoted to understand its possible cause (e.g. Mao and Wu 2008; Liu and Zhu 2016). The SCS summer monsoon onset generally occurs in mid-May, and then maximum rainfall between 110° and 120°E is located at the SCS and southeastern China (south of 25°N) until mid-June, when the maximum rainfall emerges in the middle and lower reaches of the Yangtze River basin (MLYRB), marked as the onset of the Meiyu rainy season in China (e.g. Ding and Chan 2005).

Before the SCS summer monsoon onset, southeastern China received considerable rainfall in spring (mostly in March and April), which is called as the spring persistent rainfall (Tian and Yasunari 1998; Wan and Wu 2007; LinHo et al. 2008). The spring persistent rainfall is accompanied by a convergent zone of warm and moist southwesterlies and cold and dry northwesterlies over the MLYZB. Numerical experiments demonstrate that the spring persistent rainfall would not exist without the presence of the Tibetan Plateau,

✉ Xingwen Jiang
xingwen.jiang@yahoo.com

1 Institute of Plateau Meteorology, China Meteorological Administration, 20 Guanghua Village Street, Qingyang District, Chengdu 610072, Sichuan, China

2 Heavy Rain and Drought-Flood Disasters in Plateau and Basin Key Laboratory of Sichuan Province, Chengdu, Sichuan, China

3 Laboratory for Climate Studies, National Climate Center, China Meteorological Administration, Beijing, China

4 School of Atmospheric Sciences, Sun Yat-sen University, Guangzhou, Guangdong, China

which causes low-level southwestelies over the southeastern China (Wan and Wu 2007). The southwesterlies consist of the southwesterlies generated by the Tibetan Plateau acting as a barrier for the subtropical westerlies and the southwesterlies induced by diabatic heating over the Tibetan Plateau.

Figure 1a shows seasonal evolution of latitudinal (110°–120°E) averaged rainfall, maximum rainfall belt is basically located around 27°N before it reaches to a maximum in early May, and then the maximum propagates southward. From late May to mid-June, rainfall maximum moves from the SCS northward to the MLYRB. Rainfall apparent reduces in southeastern China from mid-May to mid-June. The period with the reduction in rainfall can be regarded as the transition period from the spring persistent rainfall to the summer Meiyu. It is interesting that the reduction of rainfall starts in mid-May when the SCS summer monsoon onset occurs, and ends in mid-June when the major rain belt moves northward to the MLYRB. Mao et al. (2010) reported that the 20–50 oscillation of summer rainfall over the MLYRB varies out-of-phase with that over the SCS. Therefore, the reduction in rainfall may be linked to the SCS summer monsoon onset. Although many efforts have been made to understand the features of the stepwise northward advance of East Asian summer monsoon rainfall and associated mechanisms (e.g. Wu and Wang 2001; Ding and Chan 2005), possible links between the SCS summer monsoon onset and the spring-to-summer transition of rainfall in the MLYZB and the associated processes are not well understood.

In this study, we focused on climatological and interannual relationships between the reduction in rainfall in the MLYRB and the SCS summer monsoon onset and the underlying processes. In the rest of this paper, the data and methods used are described in Sect. 2. Main results and discussions of this study are described in Sects. 3 and 4. Finally, a summary is provided in Sect. 5.

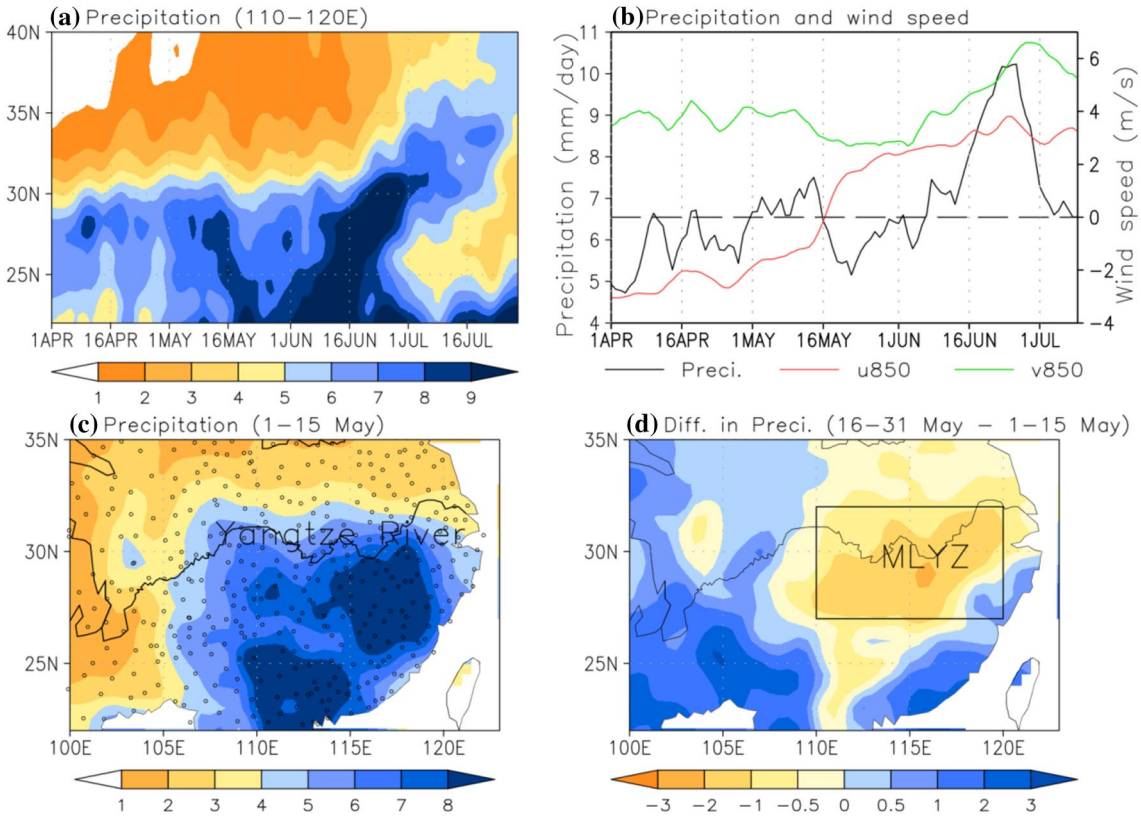

Fig. 1 **a** Latitude-time cross-sections of climatological (1961–2014) 5-day running mean precipitation (mm day^{-1}) averaged between 110°E and 120°E. **b** Time series of climatological (1961–2014) 5-day running mean precipitation (mm day^{-1}, black curve) averaged in the middle and lower reaches of the Yangtze River basin (110°–120°E, 27°–31°N, outlined by the rectangular in **d**), 850-hPa zonal wind (m s^{-1}, red curve) averaged over the South China Sea (110°–120°E, 10°–20°N), and 850-hPa meridional wind (m s^{-1}, green curve) averaged between 110°–120°E along 25°N. **c** Climatological (1961–2014) mean precipitation (mm day^{-1}, shadings) during 1–15 May, and the thick curves around 30°N denote the Yangtze River. **d** Difference in climatological mean precipitation (mm day^{-1}, shadings) between 16 and 31 May and 1–15 May

2 Data and methods

The data sets used in this study include the National Centers for Environmental Prediction–National Center for Atmospheric Research (NCEP–NCAR) reanalyses from 1961 to 2014 (Kalnay et al. 1996), Global Precipitation Climatology Project pentad precipitation dataset version 2.2 from 1979 to 2014 (Xie et al. 2011), and the gauge precipitation data (1961–2014) from the latest version (V3) of surface climatological data compiled by the China National Meteorological Information Center. Positions of the rain gauge stations are denoted by open circles in Fig. 1c.

The definition of SCS summer monsoon onset follows the operational provisions of National Climate Center, China Meteorological Administration. The SCS summer monsoon onset date is defined as the first pentad when the regional averaged 850-hPa zonal wind changes from easterlies to westerlies and the regional averaged equivalent potential temperature is higher than 340 K over 10–20°N/110–120°E and these features persist at least three consecutive pentads.

The vertically-integrated moisture flux was computed as follows:

$$\vec{Q} = \frac{1}{g}\int_{300}^{p_s} q\vec{V}dp$$

where q is the specific humidity, $\vec{V}$ the horizontal wind vector, p the air pressure, p_s the surface pressure, and g the gravitational constant. All statistical significance tests for linear correlation analysis are performed using the two-tailed Student's *t* test.

3 Results

3.1 Climatology

Figure 1b presents regional averaged 850-hPa zonal wind over the SCS. In the pentad 28 (16–20 May), zonal wind in the SCS changes from easterly wind to westerly wind and rainfall is above 6 mm day^{-1}, indicating the onset of the SCS summer monsoon according to previous studies (Wang et al. 2004). Pattern of rainfall prior to the SCS summer monsoon onset, as shown in Fig. 1c, exhibits that rainfall with considerable amount (> 6 mm day^{-1}) occurs mostly to the south of the Yangtze River. After the SCS summer monsoon onset, rainfall decreases in most of eastern China south of 35°N, except for the southeastern coast areas. The maximum reduction in rainfall (exceeding − 2 mm day^{-1}) is located mostly at the MLYZB (Fig. 1d). Seasonal evolution of the regional averaged rainfall in the MLYZB shows that the reduction in rainfall begins in mid-May and ends in mid-June (Fig. 1b). Thus, the time length of the reduction in rainfall is about 3–4 weeks.

Figure 2 shows pentad mean winds and rainfall in May. Before the SCS summer monsoon onset (11–15 May; Fig. 2a), a well formed subtropical rain belt is located at the northern edge of the western North Pacific High, stretching from southeastern China to southern Japan; the SCS is relatively dry and dominated by easterly wind. However, westerly winds prevail over the SCS in pentad 28 (16–20 May) as a result of both the eastward retreat of the western North Pacific High and the eastward development of the monsoonal westerlies from South Asia (Fig. 2b), accompanied by a significant increase in rainfall in the SCS. These features indicate the SCS summer monsoon onset occurs in pentad 28. There are no significant changes in wind and rainfall over the SCS and southern China from pentad 28 to pentad 29. The SCS summer monsoon onset is also accompanied by a significant southeastward shift of the subtropical rain belt to the south of Japan, while the ridgeline of the western North Pacific High does not exhibit evident southward shift. The differences in 15-day mean rainfall between after and before the SCS summer monsoon onset indicate that rainfall increases not only in the SCS, but also in the Bay of Bengal and the subtropical western North Pacific. On the other hand, rainfall decreases in most of northern East Asia, with maxima in the MLYZB and southern Japan.

How does the SCS summer monsoon onset cause the reduction of rainfall in the MLYZB? Compared to the atmospheric circulation prior to the SCS summer monsoon onset, there is an anomalous low-level cyclone over the subtropical western North Pacific after the SCS summer monsoon onset (Fig. 2d), which weakens the climatological mean southwesterly wind over the southern China, resulted in a weakening of northward moisture transport to the MLYZB (figures not shown). As can be seen from Fig. 1b, the reduction in the MLYZB rainfall is accompanied by a remarkable weakening of 850-hPa meridional wind averaged between 110°–120°E along 25°N from mid-May to early June. Thus, the SCS summer monsoon onset may cause the reduction in rainfall in the MLYZB by weakening the climatological low-level southwesterly moisture transport to the south of the MLYZB.

The above analyses are based on climatological mean data. To further illustrate the differences in circulation and rainfall before and after the SCS monsoon onset, we composite circulation and rainfall based on monsoon onset date for all years, which are shown in Fig. 3. The composite 850-hPa winds and rainfall further indicate that the SCS summer monsoon onset leads to remarkable increases in rainfall in the SCS and the subtropical western North Pacific, but decreases in rainfall in the MLYZB, southern Japan, and the Korean Peninsula, as well as a large anomalous cyclone

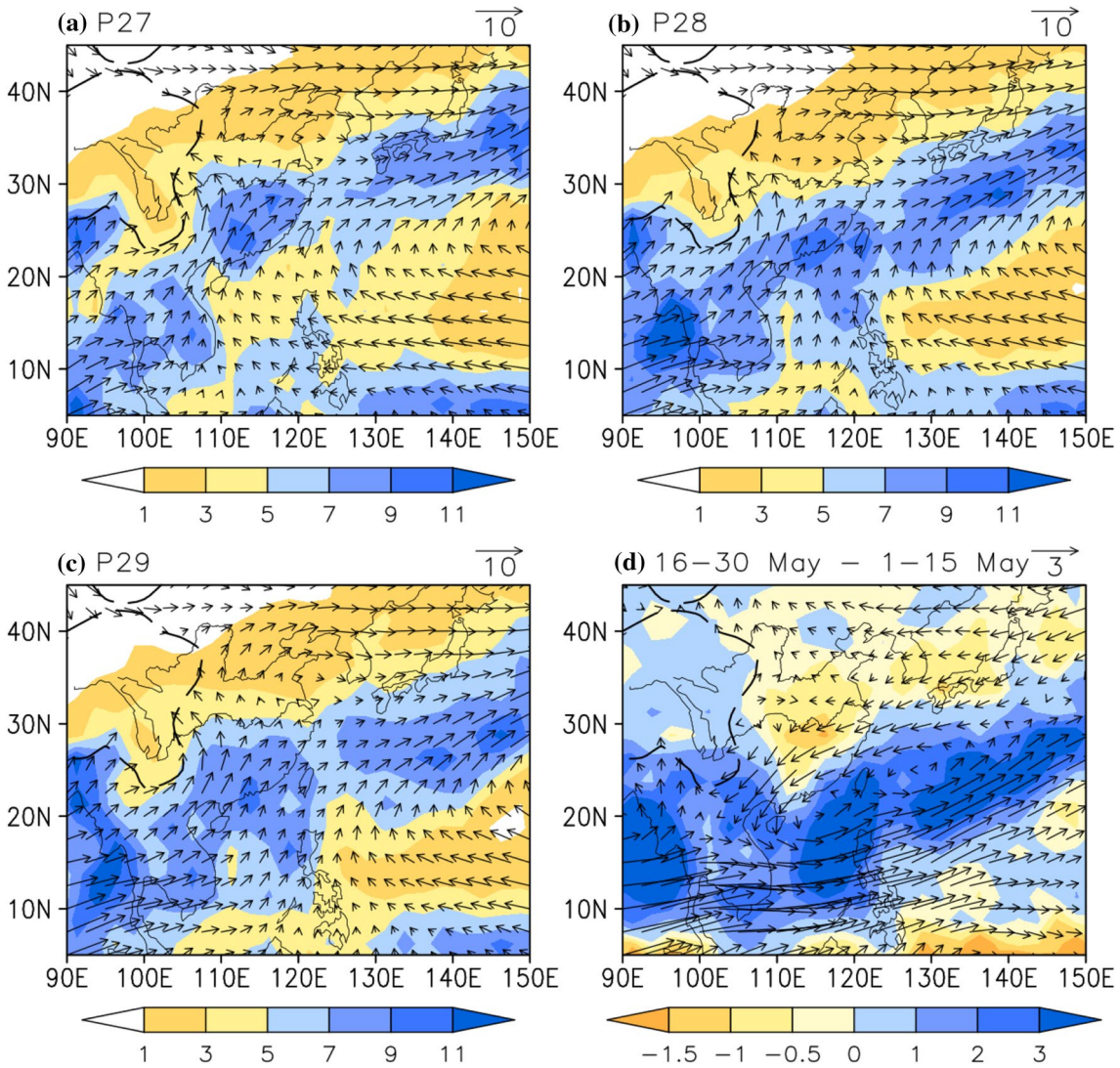

Fig. 2 Climatological pentad 850-hPa winds (m s^{-1}, vectors, 1961–2014) and precipitation (mm day^{-1}, shadings, 1979–2014) for **a** pentad 27, **b** pentad 28, and **c** pentad 29. **d** Differences in 15-day mean winds and precipitation between after (16–30 May) and before (1–15 May) the South China Sea monsoon onset

over the western North Pacific. These features are similar to those revealed by climatological mean data.

Figure 4 shows the differences in vertically-integrated moisture transport and 500-hPa vertical velocity between after and before the SCS monsoon onset. The differences in moisture transport indicate that moisture transported from the tropics to southeastern China decreases after the SCS monsoon onset, especially for the MLYZB (Fig. 4a). The differences in 500-hPa vertical velocity indicate that anomalous ascending motion occurs over the SCS and the subtropical western North Pacific, and anomalous descending motion occurs over the MLYZB (Fig. 4b). Comparisons of the differences between 500-hPa vertical velocity and rainfall indicate that anomalous ascending motion occurs over the the regions with increased rainfall, while anomalous descending motion prevails the regions with decreased rainfall. Thus, the anomalous descending motion after the SCS monsoon onset also contributes to the reduction in rainfall.

3.2 Interannual variability

Here we examine the influence of the SCS summer monsoon onset on the reduction in rainfall on interannual time scale. To obtain a stable seasonal variation of rainfall in the MLYZB, we select the years with the anomalous SCS summer monsoon onset date later or earlier than half of one standard deviation to composite the seasonal variation of rainfall for late or early SCS summer monsoon onset. The years with monsoon onset date later (earlier) than or equal to the 30th (27th) pentad is defined as late (early) monsoon

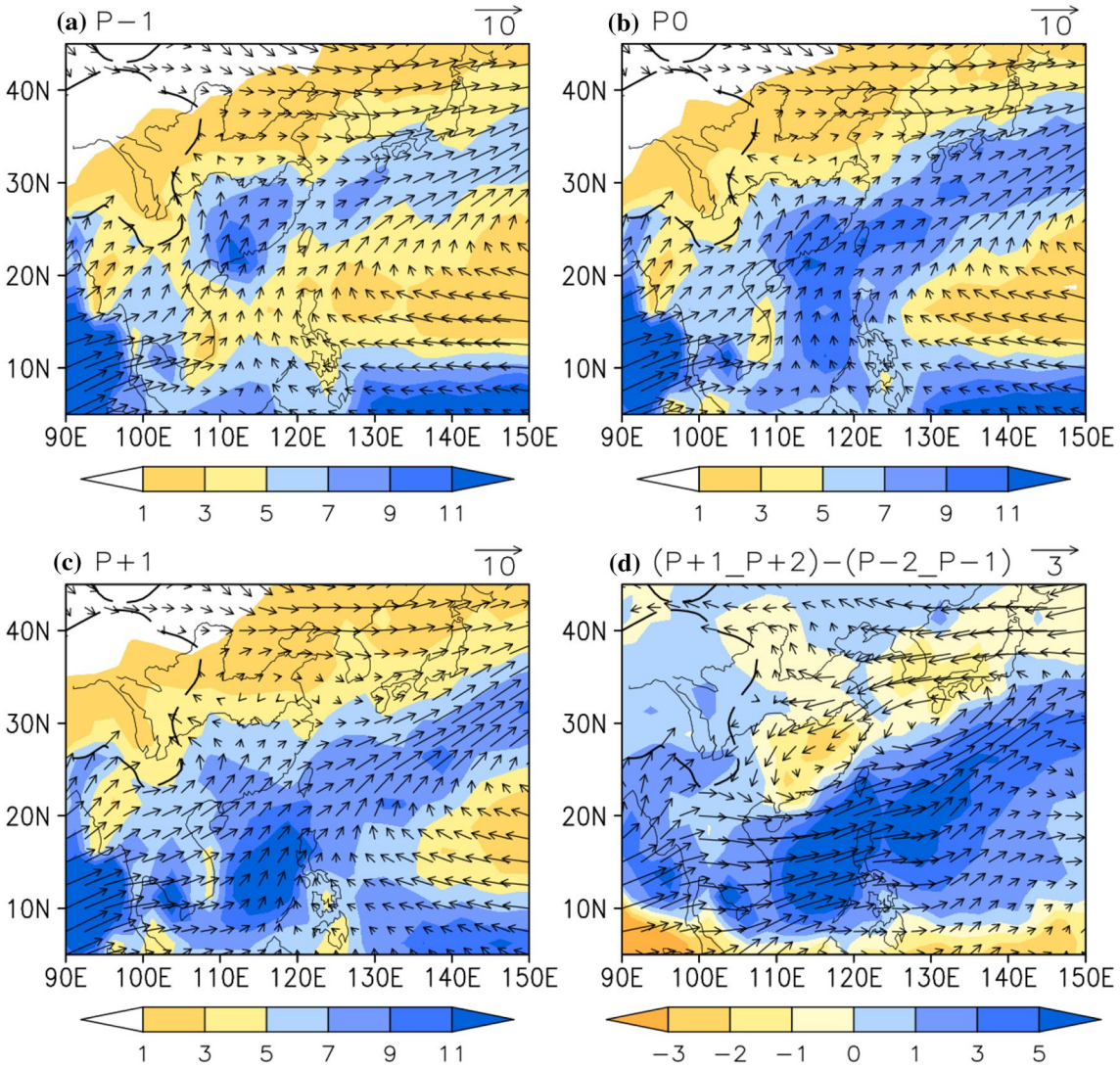

Fig. 3 Composite rainfall (mm day^{-1}, shadings, 1979–2014) and 850-hPa winds (m s^{-1}, vectors, 1961–2014) based on the SCS summer monsoon onset date for each year. **a** one pentad before the monsoon onset (P − 1), **b** during the monsoon onset (P0), **c** one pentad after the monsoon onset (P+1), and **d** two-pentad averaged differences between after (P+1_P+2) and before (P − 2_P − 1) the monsoon onset

onset years. The selected years for late or early monsoon onset are listed in Table 1. There are 16 years marked as late monsoon onset, and 13 years as early monsoon onset. Evolutions of composite variables for the late and early SCS monsoon onset years are shown in Fig. 5. The composite 850-hPa zonal wind indicates that the date of change in zonal winds from easterlies to westerlies over the SCS is different between the late and early monsoon onset years. The rainfall in the MLYZB also shows different subseasonal variations. In the early monsoon onset years, the rainfall in the MLYZB decreases persistently from early May to mid-May, and then increases and reaches to the rainfall amount before the decrease in late May. On the other hand, the rainfall in the late monsoon onset years decreases persistently from late May to mid-Jun, and then increases rapidly. These features indicate that the reduction in rainfall in MLYZB begins early (late) in the early (late) SCS summer monsoon onset years. The composite 850-hPa merdional wind to the south of MLYZB also shows an early decrease in early SCS summer monsoon onset years, consistent with the early onset of the reduction in rainfall. The meridional wind does not decrease as much as the rainfall in early June. Moreover, the start time of the decreases in both meridional wind and rainfall is several days earlier than that of the transition from easterlies to westerlies, but is corresponding to the time of the abrupt decrease in easterlies before they turn into westerlies.

The evolutions of composite rainfall over the MLYZB indicate that the differences in the timing of the reduction

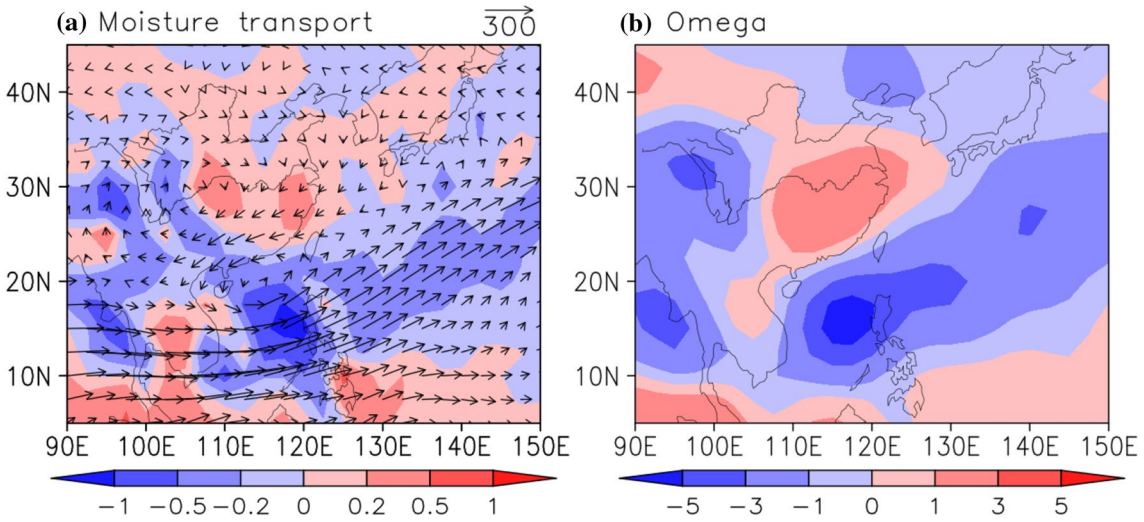

Fig. 4 Composite two-pentad averaged differences in **a** vertically-integrated moisture transport (kg m^{-1} s^{-1}; vectors) and its divergence (kg m^{-1} shadings), and **b** 500-hPa vertical velocity (0.01 Pa s^{-1}) between after (P + 1_P + 2) and before (P − 2_P − 1) the monsoon onset

Table 1 Years with the normalized value of the South China Sea monsoon onset date less than −0.5 or greater than 0.5, bold font indicates the years with the value less than −1.0 or greater than 1.0

Late onset	Early onset
1963, 1970, 1971, 1973, 1974, 1981, **1982**, 1985, **1987, 1989, 1991**, 1993, 1999, 2005, 2009, **2014**	**1966, 1972**, 1979, 1986, **1994**, 1995, **1996**, 2000, **2001**, 2002, **2008, 2011**, 2013

in rainfall could affect temporal averaged rainfall amount in May and June. For example, the rainfall amount for the early monsoon onset years is generally lower than the climatological rainfall amount in May due to early start of the reduction in rainfall; but the rainfall amount for the late monsoon onset years is generally higher than the climatological rainfall amount in late May due to late start of the reduction in rainfall. As initiative of the reduction in rainfall is modulated by the SCS monsoon onset, May rainfall in the MLYZB is positively and significantly correlated with the SCS summer monsoon onset date (Fig. 6a), with a coefficient of 0.44. The evolutions of composite rainfall also show that rainfall amount has apparent anomaly in early June for both the early and late monsoon years because of different end time of the reduction in rainfall (Fig. 5c). The SCS summer monsoon onset date is negatively correlated with June mean rainfall, with a coefficient of -0.26.

Figure 6b, c show composite differences in monthly mean rainfall and vertically-intergrated moisture transport for May between the early and late monsoon onset years. Rainfall is composited only for the years after 1979 due to the availability of the GPCP rainfall data. An early monsoon onset is accompanied by above-normal rainfall from the Bay of Bengal eastward to the western North Pacific, but below-normal rainfall over southeastern China. Strong northeasterly moisture transport anomalies are found over southeastern China in the early SCS monsoon onset years, favoring for the below-normal rainfall over southeastern China. As water vapor is mostly concentrated in the lower troposphere, the vertically-integrated moisture transport anomalies also indicate an anomalous low-level cyclone over the western North Pacific in the early SCS monsoon onset years. These differences are consistent with the differences between after and before the SCS monsoon onset (Figs. 3d, 4a), suggesting that the interannual variability of the SCS monsoon onset significantly affects May mean rainfall over not only the SCS and the subtropical western North Pacific, but also the MLYZB.

3.3 An idealized model simulation

Both the differences between the early and late monsoon years and the differences between after and before the monsoon onset years indicate that the anomalous cyclone over the western North Pacific is located to the northwest of the enhanced rainfall over the SCS and the subtropical western North Pacific. Thus, the anomalous cyclone may be explained as a response to the diabatic heating of the enhanced rainfall according to the Gill model (1980). Previous studies also indicate that diabatic heating plays an

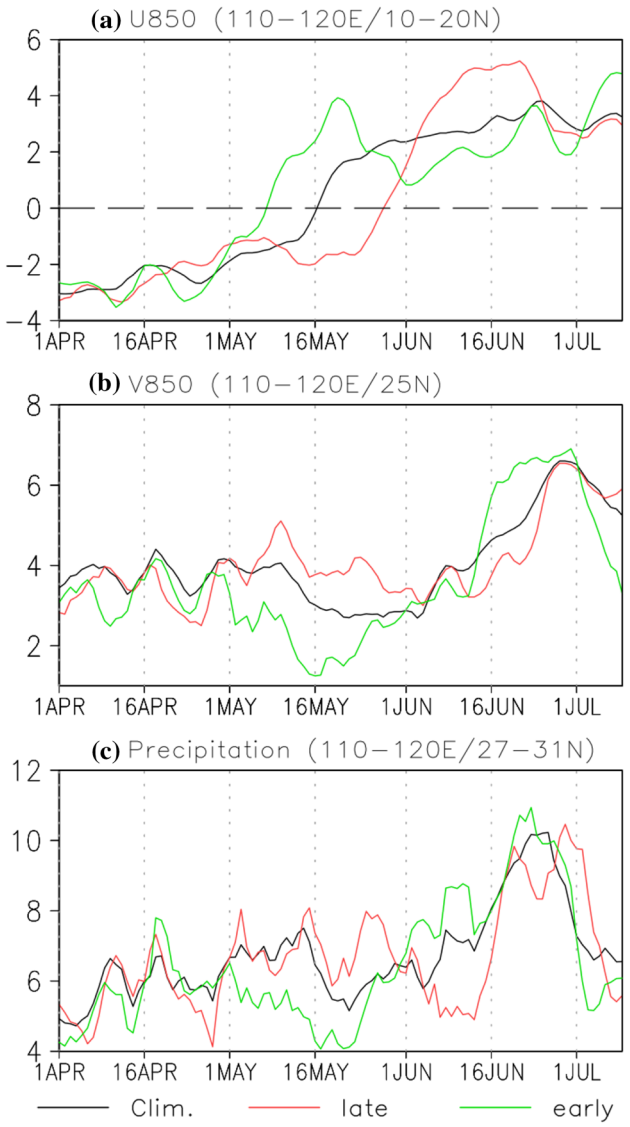

Fig. 5 Time series of 5-day running mean **a** 850-hPa zonal wind (m s^{-1}) averaged over the South China Sea (110°–120°E, 10°–20°N), **b** 850-hPa meridional (m s^{-1}) averaged between 110°–120°E along 25°N, and **c** precipitation (mm day^{-1}) averaged in middle and lower reaches of the Yangtze River basin (110°–120°E, 27°–31°N). The black, red, and green curves are composite values of all years, years with a late monsoon onset, and years with an early monsoon onset, respectively

important in circulation anomalies over East Asia (e.g. Nitta and Hu 1996).

To investigate the impacts of diabatic heating of the enhanced rainfall in the SCS and the subtropical western North Pacific on the anomalous cyclone to the northwest, a nonlinear baroclinic model, developed by Ting and Yu (1998), is employed in this study. This model is a fully nonlinear, dry, time-dependent baroclinic model with 24 sigma levels in the vertical and spectral R30 horizontal resolution. In this study, we use it to simulate atmospheric response to heating of the rainfall anomalies over the SCS and the subtropical western North Pacific with climatological zonally varying basic state taken from the ERA-interim reanalysis (Dee et al. 2011). The dissipations employed in the model include Rayleigh friction, Newtonian cooling, and biharmonic diffusion (coefficient of 1×10^{17} m^4 s^{-1}). The coefficients of Rayleigh friction and Newtonian cooling are the same, with a timescale of 0.3, 0.5, 1.0 and 8.0 days in the lowest four levels, and 15 days in the other levels. The time integration is performed for 50 days. The model solution approaches a steady state after about 15 days and the average for the last 20 days are shown in this study.

The idealized heating related to rainfall anomaly is prescribed as $Q = V(\sigma)A(\lambda, \phi)$. The vertical structure of the heating takes the form $V(\sigma) = e^{\left(-20\times(\sigma-\sigma_c)^2\right)}$. It has a maximum when σ equals σ_c and reduce to zero quickly as σ increases or decreases from σ_c. σ_c is chosen to be 0.4 in this study (Fig. 7a). The $A(\lambda, \phi)$ defines the horizontal structure and magnitude of the heating. In this study, it is depended on the differences in rainfall between after and before the SCS monsoon onset. The value of heating rate with unite of K per day equals to value of the difference in rainfall amount with unit of mm per day. Heating is limited to the region with rainfall difference higher than 2 mm per day over the SCS and subtropical western North Pacific (Fig. 7c, d). We also use rainfall amount of 1 and 3 mm per day to define the heating region, and the simulated responses are insensitive to the changes in size of the heating region.

Because the SCS monsoon onset is accompanied by increased rainfall in both the SCS and the subtropical western North Pacific, we investigate their individual and combined impacts on regional atmospheric circulation. Horizontal structure and vertical profile of the heating is shown in Fig. 7. A climatological basic state in May is used for the model simulations. The response of 850-hPa winds to the diabatic heating is presented in Fig. 7b–d. It can be seen that the heating over both the SCS and the subtropical western North Pacific can excite a cyclone to the northwest. The response of 850-hPa winds to the heating over the SCS cannot fully explain the observed anomalous northeasterlies over southeastern China. The simulated winds are similar to the observations when the heating over the subtropical western Pacific is included (Fig. 7d). Comparisons of the responses of winds to heating between the two regions indicate that the northeasterly anomalies over the MLYZB are mostly induced by the heating over the subtropical western North Pacific. It also can be seen that the responses are largely linear. The response to the combined heating is similar to the response as a sum of the responses to individual heating over the two regions (Fig. 7d, f). The linearity of the response to the heating over the tropics was also found in simulations of an atmospheric general circulation model (Schneider et al. 2003).

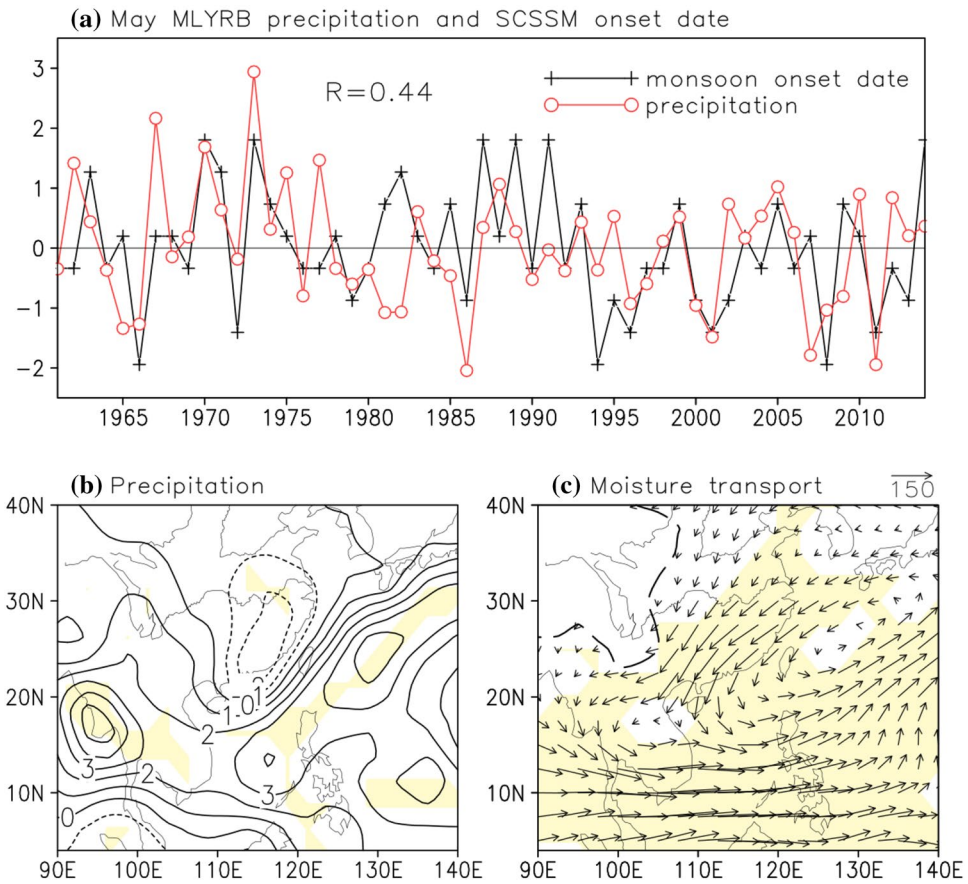

Fig. 6 **a** Time series of normalized rainfall (red lines with open circles) for May in the middle and lower reaches of the Yangtze River basin and the South China Sea monsoon onset date (black lines with pluses). Composite differences in **b** precipitation (mm day^{-1}) and **c** vertically-integrated moisture transport (kg m^{-1} s^{-1}) in May between early and late years for the South China Sea monsoon onset, values exceeding the 95% confidence level are shaded

Figure 3a shows that considerable increase in rainfall is also found over the Bay of Bengal. The wind response to this heating is presented in Fig. 7e. Compared to the wind response to heating over the SCS and the subtropical western North Pacific, the wind induced by the heating over the Bay of Bengal is weaker due to the smaller magnitude of the heating (Fig. 7b, c, e). The heating over the Bay of Bengal excites southwesterlies over southern China, which is associated with an anticyclone over the SCS and favors rainfall in the MLYZB. Thus, the heating over the Bay of Bengal is not responsible for the reduction in rainfall over the MLYZB.

As shown in Fig. 4b, after the SCS monsoon onset, there are descending motion anomalies over the MLYZB. However, the causes of the descending motion anomalies over MLYZB are unclear. Figure 8 shows the responses of 500-hPa vertical velocity to the various heating. All the simulations indicate that heating region is dominated by ascending motion, with descending motion to the northwest. As the heating moves from the SCS to the subtropical western North Pacific, the center of the descending motion also moves from central China to eastern China. Entire southeastern China is dominated by strong descending motion when heating is over both the SCS and the subtropical western North Pacific. Comparison between the simulated and observed 500-hPa vertical velocity indicates that the heating over the subtropical western North Pacific plays a more important role in descending motion over the MLYZB compared to the heating over the SCS.

The simulated responses of 200-hPa divergence indicate that there are upper-tropospheric divergences over the heating region but convergences to the northwest, where descending motion prevails. The responses of divergence and vertical velocity suggest that air over the heating region rises to the upper troposphere, and then turns to the northwest and sinks over southeastern China. The heating over the SCS and the subtropical western North Pacific could generate descending motion by inducing such vertical circulation.

All the above analyses indicate that the responses to the heating are generally a Gill-type response (Gill 1980; Liu et al. 2001) and largely linear. As a large amount of rainfall is associated with Asian monsoon, parts of the observed circulation are responses to the latent heating released by rainfall. The above simulations indicate that the main circulation changes associated with the SCS summer monsoon onset can be attributed to responses to the change in latent heating over the SCS and the subtropical western North Pacific.

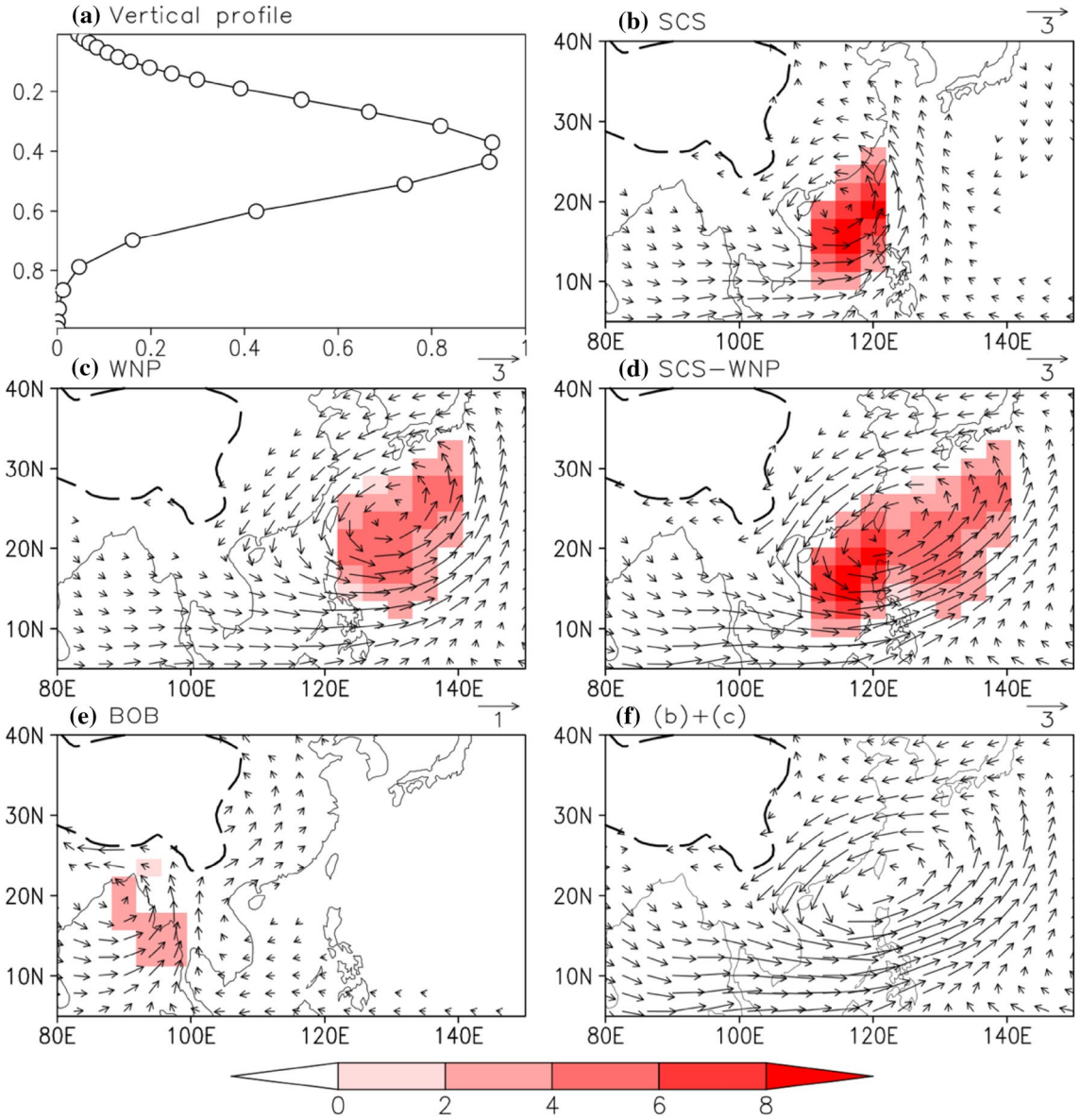

Fig. 7 **a** Vertical profile of the heating, the x-axis is magnitude of the heating (K day^{-1}) and the y-axis is height represented by sigma. The response of 850-hPa winds to heating over **b** the South China Sea, **c** the subtropical western North Pacific, **d** both the South China Sea and the subtropical western North Pacific, and **e** the Bay of Bengal. **f** is the sum of the winds in **b, c**. The heating regions and heating rate (K day^{-1}) at the sigma level of 0.6 are shown by shadings in **b–e**

4 Discussion

Figure 6a shows that the SCS summer monsoon onset experienced an interdecadal advancing after 1993/1994, while there is no evident interdecadal change in May rainfall in the MLYZB. This interdecadal change is also reflected by the years selected for composite analysis. Liu et al. (2016) reported that the monsoon onset processes are also different before and after 1993/1994. To illustrate to what extent the above composite results are influenced by the interdecadal change, we composite May rainfall and moist transport for two periods: 1961–1993 and 1994–2014. The years with the SCS summer onset date anomaly higher than one standard deviation for each period are selected to composite and listed in Table 2.

Figure 9 shows the composite differences in gauge precipitation and vertically-integrated moisture transport for the two periods. An early SCSSM onset is accompanied by suppressed rainfall in the MLYRB and an anomalous cyclone for both the two periods. Interannual variability of the rainfall in the MLYRB positively correlated with the SCSSM onset date, with correlation coefficients of 0.41 and 0.43 for

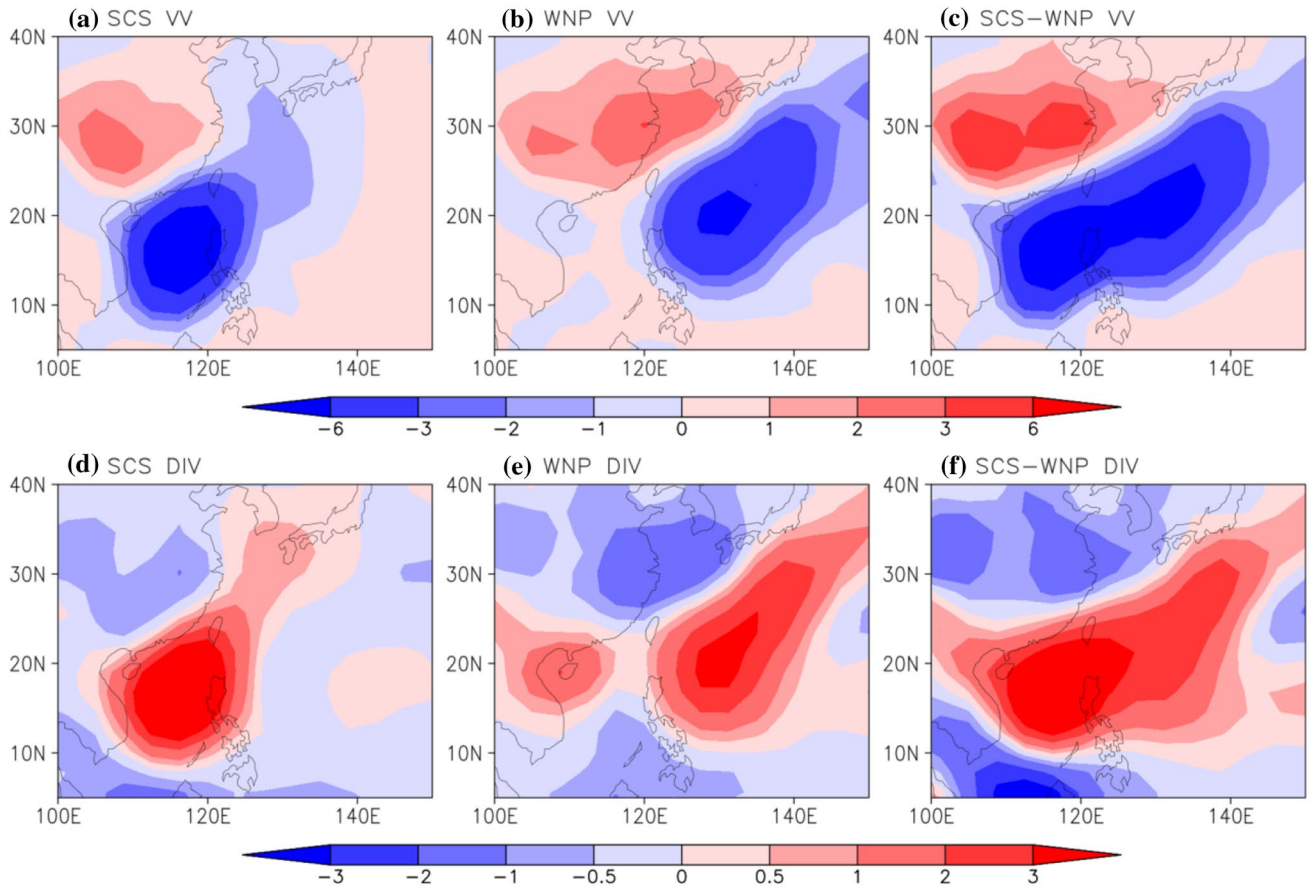

Fig. 8 The response of 500-hPa vertical velocity (10e−6 sigma s^{-1}) to heating over **b** the South China Sea, **c** the subtropical western North Pacific, and **d** both of them. **d**–**f** Are same as **a**–**c**, but for divergence (10e−6 s^{-1}). The heating regions are denoted by the shadings in Fig. 7b–d

1961–1993 and 1994–2014, respectively. Thus, the relationship of the SCSSM onset with May rainfall in the MLYRB did not have apparent interdecadal change.

Positions and magnitudes of the anomalous cyclones, however, are different between the two periods. The anomalous cyclone in the late period is weaker than that in the early period. In the early period, there are two anomalous anticyclone centers, located at the central South China Sea and the subtropical western North Pacific, respectively; but there is only one anomalous anticyclone center, located at the eastern South China Sea, in the late period. Composite GPCP precipitation also shows that spatial patterns of composite rainfall over the SCS and the western North Pacific are different between the two periods (figures not shown). These differences may be ascribed to the different processes of the SCS summer monsoon onset and the different regions where SSTs affect the SCS summer monsoon onset between the two periods (Liu et al. 2016). In spite of these differences, an early onset is always accompanied by increased rainfall over the South China Sea and the subtropical western North Pacific, which could excite the anomalous cyclone. Consequently, rainfall over the MLYZB is suppressed as the northeasterlies on the northwest of the anomalous cyclone decrease the water vapor entering to the MLYZB. Thus, an early SCS summer monsoon onset is always accompanied by suppressed rainfall over the MLYZB.

Table 2 Years with the normalized value of the South China Sea monsoon onset date less than −1.0 or greater than 1.0 for the two periods of 1961–1993 and 1994–2014

Period	Late onset	Early onset
1961–1993	1963, 1970, 1971, 1973, 1982, 1987, 1989, 1991	1966, 1972, 1979, 1986
1994–2014	1999, 2005, 2009, 2014	1994, 1996, 2001, 2008, 2011

5 Summary

The SCS summer monsoon onset has been regarded as the commencement of the East Asian summer monsoon and the rain belt migrates northward in East Asia from then on. Nevertheless, there is no increase in rainfall right after the SCS

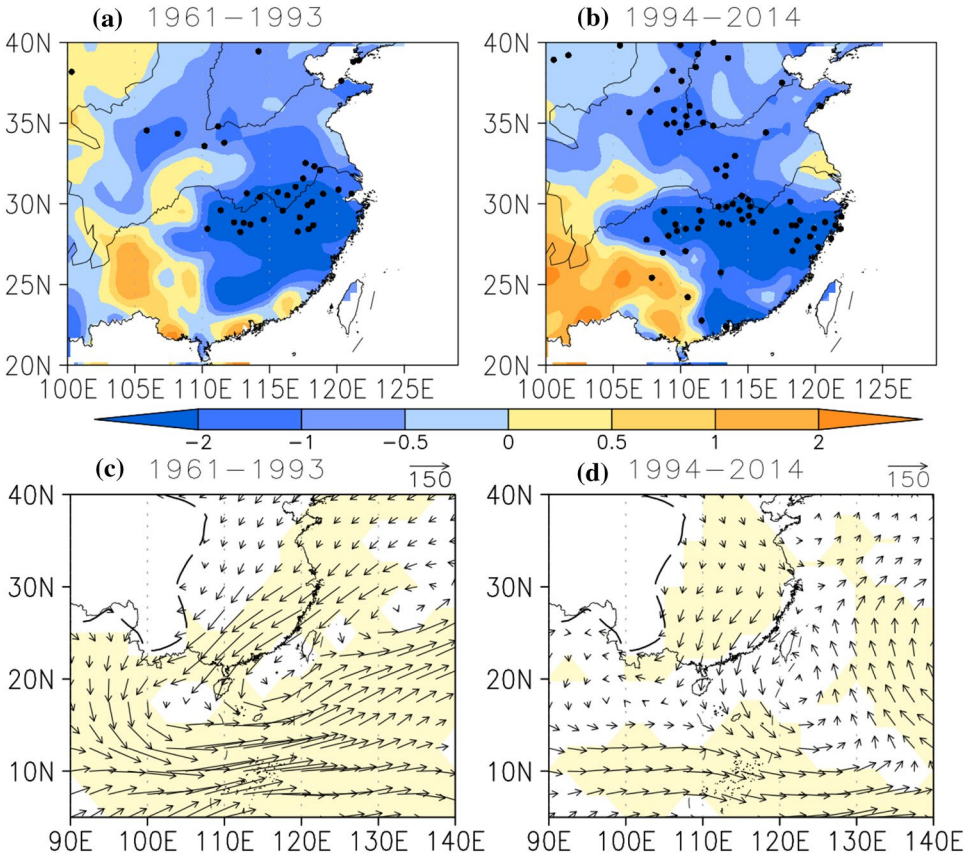

Fig. 9 Composite differences in **a** gauge precipitation (mm day^{-1}) and **c** vertically-integrated moisture transport (kg m^{-1} s^{-1}) in May between early and late years of the South China Sea monsoon onset for the period 1961–1993. **b, d** Are same as **a, c**, respectively, but for the period 1994–2014. All the years are listed in Table 2. Stippling indicates values exceeding 95% confidence level. Values exceeding the 95% confidence level are shaded in **c, d**

summer monsoon onset in subtropical East Asia. On the contrary, an apparent reduction in rainfall follows the SCS summer monsoon onset and persists for about 3–4 weeks in most of southeastern China, especially the MLYZB. The reduction in rainfall ends when the rain belt moves from the SCS to the MLYZB. There is an anomalous cyclone over the western North Pacific after the SCS monsoon onset, which weakens the southwesterlies prior to the SCS summer onset, favoring for a decrease in rainfall in the MLYZB by weakening the northward transport of moisture from the south. Anomalous descending motion also occurs over southeastern China after the SCS monsoon onset, which is another factor contributing to the reduction in rainfall in the MLYZB.

The SCS monsoon onset is accompanied by significant increase in rainfall in both the SCS and the subtropical western North Pacific, which can excite a cyclone in the lower troposphere and descending motion to the northwest. The responses to the latent heating are largely linear. Compared to the increased rainfall in the SCS, the enhanced rainfall in the subtropical western North Pacific may play a more important role in the reduction of rainfall in the MLYZB because it causes strong anomalous northeasterlies and descending motion over the the MLYZB.

As the SCS summer monsoon onset affects the initiative of the reduction in rainfall between the spring persistent rainfall and the Meiyu in the MLYZ, it can modulate the interannual variability of monthly mean rainfall in the MLYZ during May and June, especially the former. An early SCS monsoon onset is accompanied by below-normal May rainfall in the MLYZB, while a late SCS monsoon onset is accompanied by above-normal May rainfall. This relationship is robust and not affected by the interdecadal change in the SCS summer monsoon onset around 1993/1994.

Since the Asian monsoon onset features an abrupt increase in rainfall, interannual variability of monsoon onset can affect the monthly mean rainfall for May or June locally by changes in timing of the abrupt increase in rainfall (Xing et al. 2016). Because the monsoon onset is accompanied by large increase in rainfall, the associated enhanced latent heating leads to considerable change in regional circulation and rainfall nearby. This study found that the SCS summer monsoon onset affects the reduction of rainfall in the MYLZB as well as interannual variability of May mean rainfall. As current dynamical model has better skill for subseasonal prediction of rainfall in the tropics compared to that in the extratropics, subseasonal prediction of rainfall over the MLYZB around May may be improved based the dynamical prediction of the SCS summer monsoon onset and the findings in this study.

Acknowledgements The authors thank Prof. Mingfang Ting for providing the nonlinear baroclinic model. This study was jointly supported by the National Natural Science Foundation of China (Grants 41661144019), the National Key Research and Development Program (2016YFA0601502), the Basic Research and Operation Program of the CMA Institute of Plateau Meteorology (BROP 201514).

References

Dee DP, Uppala SM, Simmons AJ et al (2011) The ERA-Interim reanalysis: configuration and performance of the data assimilation system. Q J R Meteorol Soc 137:553–597

Ding Y, Chan JCL (2005) The East Asian summer monsoon: an overview. Meteorol Atmos Phys 89:117–142

Ding RQ, Ha KJ, Li JP (2010) Interdecadal shift in the relationship between the East Asian summer monsoon and the tropical Indian Ocean. Clim Dyn 34:1059–1071

Gill A (1980) Some simple solutions for heat-induced tropical circulations. Q J R Met Soc 106:447–462

Kalnay E et al (1996) The NCEP/NCAR 40-year reanalysis project. Bull Am Meteorol Soc 77:437–471

Li J, Wu Z, Jiang Z, He J (2010) Can global warming strengthen the East Asian summer monsoon? J Clim 23:6696–6705

LinHo LH, Huang XL, Lau NC (2008) Winter-to-spring transition in East Asia: a planetary-scale perspective of the south China spring rain onset. J Clim 21:3081–3096

Liu BQ, Zhu C (2016) A possible precursor of the South China Sea summer monsoon onset: effect of the South Asian High. Geophys Res Lett 43(20):11072–11079

Liu Y, Wu G, Liu H, Liu P (2001) Condensation heating of the Asian summer monsoon and the subtropical anticyclone in the Eastern Hemisphere. Clim Dyn 17(4):327–338

Liu BQ, Zhu CW, Yuan Y, Xu K (2016) Two types of interannual variability of South China Sea summer monsoon onset related to the SST anomalies before and after 1993/94. J Clim 29:6957–6971

Mao J, Wu GX (2008) Influences of Typhoon Chanchu on the 2006 South China Sea summer monsoon onset. Geophys Res Lett 35:L12809

Mao JY, Sun Z, Wu GX (2010) 20–50-day oscillation of summer Yangtze rainfall in response to intraseasonal variations in the subtropical high over the western North Pacific and South China Sea. Clim Dyn 34:747–761

Nitta T, Hu ZZ (1996) Summer climate variability in China and its association with 500 hPa height and tropical convection. J Meteorol Soc Jpn 74:425–445

Schneider EK, Bengtsson L, Hu ZZ (2003) Forcing of Northern Hemisphere climate trends. J Atmos Sci 60:1504–1521

Tao S, Chen L (1987) A review of recent research on the East Asian summer monsoon in China. In: Chang CP, Krishnamurti TN (eds) Monsoon meteorology. Oxford University Press, Oxford, pp 60–92

Tian S, Yasunari T (1998) Climatological aspects and mechanism of spring persistent rains over central China. J Meteorol Soc Jpn 76:57–71

Ting M, Yu L (1998) Steady response to tropical heating in wave linear and nonlinear baroclinic models. J Atmos Sci 55:3565–3582

Wan R, Wu GX (2007) Mechanism of the spring persistent rains over southeastern. China Sci China 50D:130–144

Wang B, LinHo, Zhang Y, Lu MM (2004) Definition of South China Sea monsoon onset and commencement of the East Asia summer monsoon. J Clim 17:699–710

Wu R, Wang B (2001) Multi-stage onset of the summer monsoon over the western North Pacific. Clim Dyn 17:277–289

Xie P, Adler RF, Huffman GJ, Bolvin D (2011) Global precipitation climatology project—Pentad, Version 2.2. NOAA National Climatic Data Center

Xing N, Li J, Wang L (2016) Effect of the early and late onset of summer monsoon over the Bay of Bengal on Asian precipitation in May. Clim Dyn 47:1961–1970